

A NOVEL FOUR LAYER METALLIZATION FOR MICROWAVE INTEGRATED CIRCUITS

R. K. Sharma^{*}, S. Patel, A. Bindal, and K. C. Pargaien

Space Applications Centre, Ahmedabad 380015, India

Abstract—In order to overcome the problems facing Cr-Cu-Au metallization, such as discoloration, diffusion of Cu into Au, a four-layer metallization Cr-Cu-NiP-Au is demonstrated on alumina substrate for microwave integrated circuit (MICs). A amorphous and nonmagnetic NiP barrier layer is used to avoid the diffusion of Cu into Au through the grain boundaries, which are the low activation energy path for diffusion at moderate temperature.

In this view, properties of Cr-Cu-NiP-Au metallization, such as sheet resistance, solderability, bondability and adhesion strength, are evaluated. Further integrity of Cr-Cu-NiP-Au structure is evaluated by subjecting to this structure to multiple temperature cycles test. Visual observation is carried out before and after the thermal cycling test. No degradation is observed as the consequence of thermal cycling test. Test and evaluation are carried out for a multi-section broadband power divider (1 : 2) on this metallization (metal thickness 12–12.5 microns) in the 0–6 GHz frequency range. Insertion loss, return loss and isolation are comparable with Cr-Cu-Au (metal thickness 5.0–6.0 microns). Performance of the power divider and properties of this metallization system reveal its novelty over the existing.

1. INTRODUCTION

Microwave Integrated Circuits are an important element of the subsystems of communication and microwave remote sensing payloads. The fabrication process of MIC starts with metallization. Therefore, metallization of the substrate is an important aspect of fabrication of microwave integrated circuits [1]. Metallization is a well-developed technology for the fabrication of integrated circuits based on silicon

Received 6 December 2011, Accepted 31 January 2012, Scheduled 7 February 2012

* Corresponding author: Rakesh Kumar Sharma (rakeshs@sac.isro.gov.in).

substrates and microwave integrated circuits based on alumina substrates, etc. There are a number of metallization systems, such as Cr-Cu-Au, Cr-Au, and TiW-Ni-Au, over bare alumina substrate. Sputtering and vacuum evaporation processes are used for the metallization. Electro-deposition or other processes may be used to further increase metallization thickness. Each of these metallization systems has both merits and demerits.

Copper and gold, highly conducting metals, are widely used in the semiconductor industry and elsewhere [2]. Copper is a promising interconnect material because of its lower electrical resistivity (bulk, $1.67 \mu\text{ohm-cm}$) and higher resistance against electromigration than aluminum and its alloys [3]. A possibility to increase materials performance for different applications is to protect them by coating. Thin gold coating is used over copper surface to prevent oxidation of the copper because gold does not oxidize but dissolves into the solder materials. However, gold cannot be plated directly onto the copper because copper would diffuse into the gold and form an easily oxidable compound [4]. Moreover, even at a temperature as low as 200°C , copper diffuses into gold, which deteriorates the performance [5]. Therefore, it is necessary to insert a barrier between copper and gold to isolate the copper so that gold can be directly plated on the top of barrier layer in order to reduce the limitations of the sputtering and vacuum evaporation processes [6]. In addition, barriers must not only be successful in retarding the copper diffusion but also have good adhesion performance, solderability, and bondability. Electroless nickel immersion gold finish is a widely used process in many industries, including microelectronics and printed circuit board manufacturing to protect the copper circuit from oxidation [7]. This process is simple and requires fewer chemicals and less machine maintenance. Without any metal waste, both sides of the substrate can be coated in one operation. Thus, total time required to coat a substrate is considerably less than that in the sputtering and vacuum evaporation processes.

The aim of the present work is to study the properties of this metallization system, such as sheet resistance, adhesion strength, solderability, bondability and effect of the thermal cycling test. In order to evaluate the microwave behavior of this metallization for MIC's, a multi-section broadband power divider has been fabricated. A comparative study of the microwave losses in microstrip configuration for multi-section broadband power divider realized on this metallization and on Cr-Cu-Au metallized alumina substrate has been carried out.

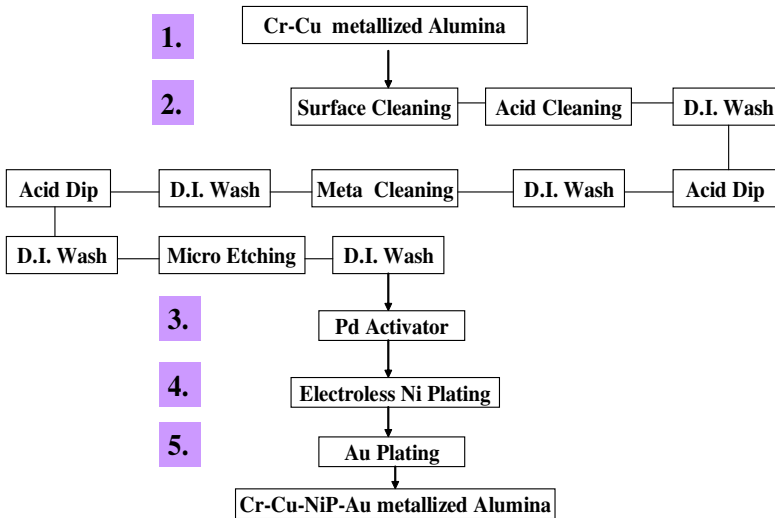


Figure 1. Flow chart for electroless Ni and Au plating.

2. EXPERIMENTAL METHOD

Electroless technique is used for nickel deposition. This is a complex technique and requires surface activation by a Pd. In the conventional technique, nickel ions are formed as a result of reduction of nickel solution in the presence of a catalyst (viz., Pd). Prior to metallization of electroless nickel, Cr-Cu metallized substrates were cleaned sequentially as given in the Figure 1. Thin nickel film (0.5–5.0 μ) was deposited on the cleaned and micro-etched surfaces of Cr-Cu metallized alumina substrate. Subsequently, a gold layer (1.5–2. μ) was deposited by using non-cyanide gold bath at a temperature of 95–98°C. These metallized substrates were annealed at 180°C in ambient for one, two and three hours.

3. RESULTS AND DISCUSSION

3.1. Thickness Measurement

Thickness of all the samples was measured by coating measuring instrument, based on XRF principle at SAC. Uniform plating is obtained. Results are given in Table 1.

Table 1. Thickness of Cu, NiP, and Au in Cr-Cu-NiP-Au metallized alumina substrate.

Sample No	Thickness in Micron				
	Cu Thickness	NiP		Au	
		Plating Time In minute	Thickness	Plating Time In minute	Thickness
1	1.72	5	0.70	25	1.89
2	1.67	10	1.38	25	2.02
3	1.70	15	2.18	25	1.89
4	1.06	20	2.90	25	2.00
5	1.30	25	3.38	25	1.91
6	1.20	35	4.40	25	1.90

3.2. Thermal Cycling Test (TCT)

To evaluate the thermal stability of this metallized structure, thermal cycling test was carried out in accordance with MIL-STD-883. Graphical representation of TCT is given in Figure 2. Specifications for thermal cycling test are given below:

Min Temp: -65°C

Max Temp: 150°C

Dwell time: 10 min each

No. of cycles: 100 cycles

Total Transfer Time ≤ 1 minute

Specified Temp reached in ≤ 15 minutes

3.3. Sheet Resistivity Measurement

Sheet resistivity of all samples was measured by DC four-probe method before and after the thermal cycling test (TCT) as well as after annealing. The results are given in Table 2.

Sheet resistivity before and after the thermal cycling and annealing remains the same or decreases because of improvement in the crystallinity. Since sheet resistivity is not increasing as the consequence of thermal cycling and annealing, Cu is not diffusing into Au. It means that NiP is acting as an effective barrier layer for Cu diffusion.

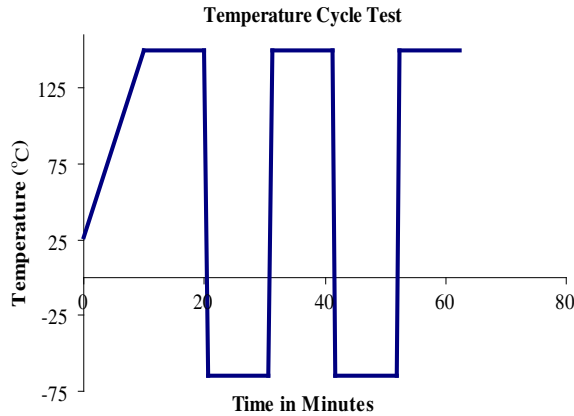


Figure 2. Graphical representation of TCT.

Table 2. Sheet resistivity of Cr-Cu-NiP-Au metallized alumina before and after TCT.

Thickness in Micron			Sheet Resistivity (SR) in Ohms/square				
Cu	NiP	Au	Before	After TCT	after annealing at 180°C		
					Time minute		
					60	120	180
1.72	0.70	1.89	0.0045	0.0042	0.0045	0.0044	0.0044
1.67	1.38	2.02	0.0040	0.0041	0.0039	0.0039	0.0039
1.70	2.18	1.89	0.0046	0.0047	0.0044	0.0046	0.0045
1.06	2.90	2.00	0.0050	0.0045	0.0048	0.0047	0.0049
1.20	4.40	1.90	0.0042	0.0045	0.0035	0.0042	0.0039

3.4. Visual Inspection

Visual inspection was carried out before and after annealing as well as after the thermal cycling test. No degradation and visibility of Cu and NiP have been observed as the consequence of thermal cycling test and annealing.

3.5. Adhesion Test

Adhesion was tested destructively after engraving the adhesion pattern by stud pull test method. It was found that adhesion strength for Cr-Cu-NiP-Au metallized substrate is greater than 590 Kg/cm² because epoxy failure occurs for the force 33.59 Kg, but pad remains as it is.

Therefore, this metallization shows the excellent adhesion according to the MIL-STD-883.

3.6. Bondability Test

Bond strength was tested for 20-mil ribbon bond by pull test method. Ribbons were bonded by parallel gap method. It was found that bond strength of 20 mil gold ribbon is greater than 100 gm. Pull test and visual inspection imply that this metallized substrate meets the ribbon bonding criteria according to the MIL-STD-883.

3.7. Solderability Test

With the trend of miniaturization of electronic devices, the electronic industry faces many new challenges. Solder joint reliability is one of them. Wetting balance analysis, a quantitative test, was used to characterize the wettability. It measures the wetting forces imposed by the molten solder on the test surface as metallized substrate is dipped into and held in the solder bath as a function of time. This metallization passes this test and shows excellent wettability hence solderability.

To evaluate the solder joint strength, die-shear test is also carried out on capacitor (CDR2) mounted on conducting pads of MICs fabricated on substrate by reflow soldering method. Solder joint strength is found to be 3.7836 Kg while required 0.9 Kg according to the MIL-STD-883, Cr-Cu-NiP-Au metallization show excellent solder joint strength. The result is shown in Table 3.

Table 3. Result of die shear test of Cr-Cu-NiP-Au metallized alumina substrate.

Force in Kg	Termination Area	Mil Std. value
3.7836	9.428×10^{-4}	0.9 Kg

3.8. Microwave Characterization

To characterize losses, a multi-section broadband Wilkinson power divider was fabricated on the Cr-Cu-NiP-Au metallized alumina substrate. Fabricated multi-section broadband Wilkinson power divider on Cr-Cu-NiP-Au metallized alumina substrate and its layouts are shown in Figure 3 and Figure 4, respectively. The dimension of the broadband Wilkinson power divider is 25 mm * 14 mm, so the whole micro stripe circuit is confined within a 1 inch * 1 inch substrate.

The size of the resistor is 2.5 mm * 1.2 mm. The design details are described somewhere else [8]. A two-port network analyzer along with an attenuator of 60-dB (with a characteristic impedance 50 ohms for third port) was used in this experiment. Isolation, insertion, and return loss were measured across a range of frequencies (0 to 6 GHz) in decibels. Input ($|S_{11}|$)/output return loss ($|S_{22}|$) and insertion loss ($|S_{21}|$) were measured by connecting the input port of the power divider to the input of network analyzer and one of the output port (port number 2) of the power divider to the output port of network analyzer while keeping the second output port (port number 3) of the power divider attenuated by using an attenuator of 60-dB. S_{11} ,

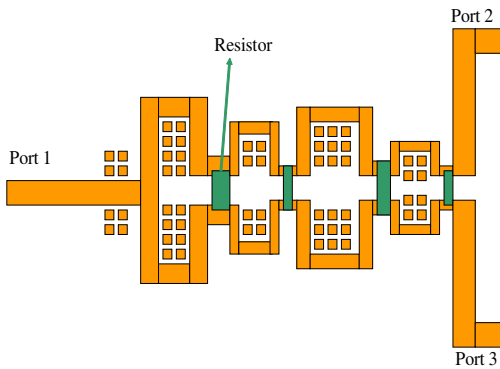


Figure 3. Layouts of the multi-section broadband Wilkinson power divider.

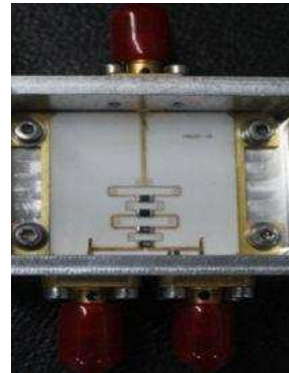


Figure 4. Broadband power divider realized on Cr-Cu-NiP-Au metallized Alumina.

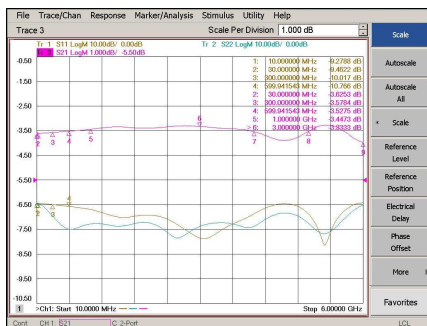


Figure 5. S_{11} , S_{22} and S_{21} vs. frequency.

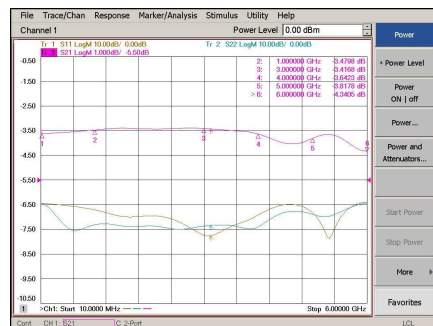


Figure 6. S_{11} , S_{33} and S_{31} vs. frequency.

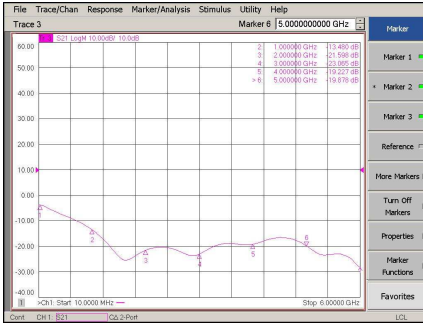


Figure 7. S_{23} vs. frequency.

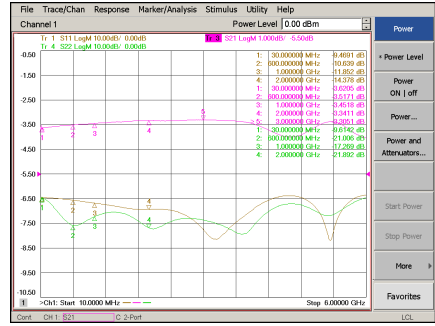


Figure 8. S_{11} , S_{22} and S_{21} vs. frequency.

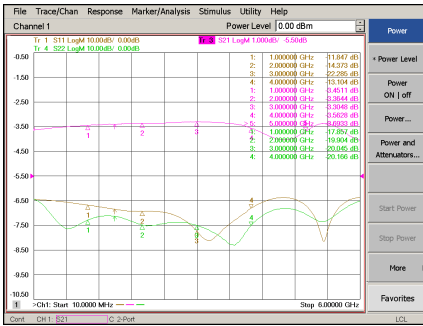


Figure 9. S_{11} , S_{33} and S_{31} vs. frequency.

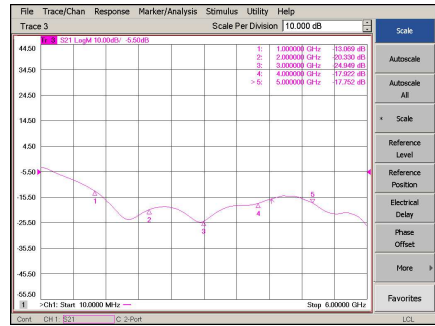


Figure 10. S_{23} vs. frequency.

S_{22} , and S_{21} are presented as dB vs. GHz as shown in Figure 5. Input ($|S_{11}|$)/output return loss ($|S_{33}|$), and insertion loss ($|S_{31}|$) were measured by connecting the output port of network analyzer to port number 3 and attenuator to port number 2. S_{11} , S_{33} , and S_{31} are presented as dB vs. GHz as shown in Figure 6 (in figure number 6, S_{22} is S_{33} , and S_{21} is S_{31}). Isolation ($|S_{23}|$ that in our experiment is $|S_{21}|$) was measured by connecting both output ports 2 and 3 of the power divider to both the ports of network analyzer and putting attenuator to port 1. S_{23} is presented as dB vs. GHz as shown in Figure 7. Input/output return loss, insertion loss data, and isolation ($|S_{23}|$) were compared for the same power divider realized on Cr-Cu-Au metallized alumina substrate and given in Table 4. S_{11} , S_{22} and S_{21} for Cr-Cu-Au metallization are presented as dB vs. GHz as shown in Figure 8 while S_{11} , S_{33} and S_{31} in Figure 9 (in figure number 9, S_{22} is S_{33} , and S_{21} is S_{31}). Isolation for Cr-Cu-Au metallization is shown in Figure 10.

From Figure 5 and Figure 6, we can observe insertion loss value 3.3478 dB at the centre frequency 2.5 GHz and bandwidth of 4 GHz (0.5–4.5 GHz) approximately. Amplitude imbalance $\text{abs}(S_{21}-S_{31})$ and phase imbalance $\text{abs}(\text{phase}(S_{21})-\text{phase}(S_{31}))$ are approximately the same as that realized on Cr-Cu-Au metallized alumina substrate. From this experiment, we conclude that the presence of NiP in between Cu and Au does not degrade the performance of broadband power divider. In future, experiments and test specimen will be refined to collect more comprehensive data. The test specimen will include resonator structures that will allow differentiation among conductor and dielectric losses.

Table 4. Comparison of input/ output return loss, insertion loss and isolation.

Frequency	Input return loss ($ S_{11} $) in dB		Output return loss ($ S_{22} $) in dB		Insertion loss ($ S_{21} $) in dB		Isolation ($ S_{23} $) in dB	
	Cr-Cu-Au	Cr-Cu-NiP-Au	Cr-Cu-Au	Cr-Cu-NiP-Au	Cr-Cu-Au	Cr-Cu-NiP-Au	Cr-Cu-Au	Cr-Cu-NiP-Au
600 MHz	10.639	10.766	21.006	22.975	3.5171	3.5275	8.6962	8.9268
1 GHz	11.852	12.143	17.269	18.078	3.4518	3.4473	13.069	13.480
2 GHz	14.378	14.386	21.892	20.126	3.3411	3.3976	20.330	21.598
3 GHz	22.285	22.367	20.045	19.056	3.3051	3.3333	24.949	23.065
4 GHz	13.033	13.987	19.220	19.158	3.5369	3.5462	17.922	19.227
5 GHz	12.060	13.107	14.375	14.347	3.6817	3.5462	17.752	19.978
6 GHz	9.4691	9.4387	9.6142	9.316	4.0350	4.0893	26.839	28.369

4. CONCLUSIONS

Thin NiP films of different thicknesses were obtained successfully to keep the gold plating thickness constant. Visual inspection carried out for all the samples implies that plating thickness is uniform. This metallization Cr-Cu-NiP-Au passed thermal cycling test. Besides, sheet resistivity remains the same or improved, which implies that Cu diffusion does not occur in Au layer and that NiP acts as a good effective barrier layer for Cu diffusion.

Cr-Cu-NiP-Au metallized substrate shows excellent adhesion, bondability, wettability, and solderability. No degradation was observed in performance of the multi-section power divider realized on Cr-Cu-NiP-Au (thickness 12–12.5 micron) metallized substrate in comparison with Cr-Cu-Au metallization (thickness 5–6 micron) in

terms of insertion loss, return loss. NiP not only works as effective barrier layer but also improves adhesion, bondability, wettability and solderability excellently when it is inserted in between Cu and Au in Cr-Cu-Au metallization structure.

ACKNOWLEDGMENT

The authors would like to thank Shri D. Bala Subrymanyam DD ESSA, Shri Asit Battacharya GH ESSA, Shri R. S. Sharma Head MEAD, Shri V. V. Limaye, Head STPD, Shri M. M. Vachhani Head QAPD, Shri M. P. Gondaliya Head DAPF, Shri R. B. Upadhyay Head TSPD for providing support and facility whenever required for carrying out this project and Pankaj Jain for microwave characterization.

Authors also would like to thank Shri Rajkumar Arora DD, ESSA and Shri Apurba Bhattacharya GD MEG for their motivation and encouragement.

REFERENCES

1. Puri, V., "Effect of metallization process on the performance of passive microstripline circuits," *Microwave and Optical Technology Letters*, Vol. 5, No. 11, 585–590, 1992.
2. Abel, L., et al. edited, *Electronic Materials Handbook*, Vol. 1, Packaging, ASM International, 1989.
3. Plummet, J. D., M. D. Deal, and P. B. Griffin, *Silicon VLSI Technology*, 695, Upper Saddle River, Prentice Hall, NJ, 2000.
4. Alternative Board Finishes, *A Publication of the National Electronic Manufacturing Center of Excellence, Electronic Manufacturing Productivity Facility (EMPF)*, 49, 2000.
5. Diamand, Y. S., et al., *Proc. 9 Bienn. Univ. Gov. Ind. Microelectron. Symp.*, 210–215, IEEE, Piscataway, NJ, 1991.
6. Mahapatra, S. and S. N. Prasad, "A new electroless method for low loss microwave integrated circuits," *IEEE Trans. Components, Hybrids Manuj. Technol.*, Vol. 1, No. 4, Dec. 1978.
7. Coombs, Jr., C. F., *Printed Circuit Handbook*, 5th Edition, 1400, McGraw-Hill, New York, United States, 2001.
8. Kishihara, M., et al., "A design of multi-stage, multi-way microstrip power dividers with broadband properties," *IEEE MTT-S Digest*, 2004.